



Reduced Nitrous Oxide Emissions From Drained Temperate Agricultural Peatland After Coverage With Mineral Soil

Yuqiao Wang^{1,2*}, Sonja M. Paul¹, Markus Jocher¹, Christine Alewell² and Jens Leifeld^{1,2}

¹Climate and Agriculture Group, Agroscope, Zürich, Switzerland, ²Environmental Geosciences, University of Basel, Basel, Switzerland

OPEN ACCESS

Edited by:

Rosa Francaviglia,
Council for Agricultural and
Economics Research (CREA), Italy

Reviewed by:

Ülo Mander,
University of Tartu, Estonia
Nicola Dal Ferro,
University of Padua, Italy

*Correspondence:

Yuqiao Wang
yuqiao.wang@agroscope.admin.ch

Specialty section:

This article was submitted to
Soil Processes,
a section of the journal
Frontiers in Environmental Science

Received: 17 January 2022

Accepted: 10 February 2022

Published: 03 March 2022

Citation:

Wang Y, Paul SM, Jocher M, Alewell C
and Leifeld J (2022) Reduced Nitrous
Oxide Emissions From Drained
Temperate Agricultural Peatland After
Coverage With Mineral Soil.
Front. Environ. Sci. 10:856599.
doi: 10.3389/fenvs.2022.856599

Peatlands drained for agriculture emit large amounts of nitrous oxide (N₂O) and thereby contribute to global warming. In order to counteract soil subsidence and sustain agricultural productivity, mineral soil coverage of drained organic soil is an increasingly used practice. This management option may also influence soil-borne N₂O emissions. Understanding the effect of mineral soil coverage on N₂O emissions from agricultural peatland is necessary to implement peatland management strategies which not only sustain agricultural productivity but also reduce N₂O emissions. In this study, we aimed to quantify the N₂O emissions from an agriculturally managed peatland in Switzerland and to evaluate the effect of mineral soil coverage on these emissions. The study was conducted over two years on a grassland on drained nutrient-rich fen in the Swiss Rhine Valley which was divided into two parts, both with identical management. One site was not covered with mineral soil (reference “Ref”), and the other site had a ~40 cm thick mineral soil cover (coverage “Cov”). The grassland was intensively managed, cut 5–6 times per year, and received c. 230 kg N ha⁻¹ yr⁻¹ of nitrogen fertilizer. N₂O emissions were continuously monitored using an automatic time integrating chamber (ATIC) system. During the experimental period, site Ref released 20.5 ± 2.7 kg N ha⁻¹ yr⁻¹ N₂O-N, whereas the N₂O emission from site Cov was only 2.3 ± 0.4 kg N ha⁻¹ yr⁻¹. Peak N₂O emissions were mostly detected following fertilizer application and lasted for 2–3 weeks before returning to the background N₂O emissions. At both sites, N₂O peaks related to fertilization events contributed more than half of the overall N₂O emissions. However, not only the fertilization induced N₂O peaks but also background N₂O emissions were lower with mineral soil coverage. Our data suggest a strong and continued reduction in N₂O emissions with mineral soil cover from the investigated organic soil. Mineral soil coverage, therefore, seems to be a promising N₂O mitigation option for intensively used drained organic soils when a sustained use of the drained peatland for intensive agricultural production is foreseen, and potential rewetting and restoration of the peatland are not possible.

Keywords: organic soil, mineral soil coverage, peatland management, fertilizer, GHG mitigation

1 INTRODUCTION

Nitrous oxide (N₂O) is the third most important long-lived greenhouse gas (GHG) and also an important reactant with stratospheric ozone (Ravishankara et al., 2009; Prather et al., 2015). In the last centuries, N₂O emission increased from ~12 Tg N yr⁻¹ in the preindustrial period to ~19 Tg N yr⁻¹ (Syakila and Kroeze, 2011). To a large extent, the rapid increase in N₂O emissions is driven by soil-borne N₂O, which increased from ~6.3 Tg N yr⁻¹ to ~10 Tg N yr⁻¹ over the same period, accounting for ~53% of the total N₂O increase (Tian et al., 2019). Therefore, lowering soil N₂O emission is of great importance for global N₂O mitigation, and consequently for meeting the climate target.

Peatlands only account for 3% of the terrestrial land surface but store around 644 Gt organic carbon (C) (Yu et al., 2010). Peatlands are also an important pool of organic nitrogen (N) of 8–15 Gt N (Leifeld and Menichetti, 2018). To date, more than 10% of the global peatland areas have been drained for agriculture and forestry, with a much higher share in some European countries, where around half of the peatlands are artificially drained to enhance agricultural and forest productivity in Europe, and even ~90% in Switzerland (Bragg et al., 2013; Wüst-Galley et al., 2015; Kasimir et al., 2018). However, long-term drainage causes peatland subsidence due to physical processes and mineralization of the surface peat. These processes cause soil degradation and induce very high GHG emissions, which turned the global peatland biome from a net GHG sink to a net source. It has been estimated that with the ongoing peatland degradation, c. 2.3 Gt N will be released globally (Leifeld and Menichetti, 2018). In Europe, peatland management induces N₂O emission of c. 145 Gg N yr⁻¹ (Liu et al., 2020). Full peatland restoration or other steps involving rewetting decrease the peat oxidation by re-raising the water table (Blodau, 2002) and might save substantial parts of the N mineralization and also halt peatland subsidence (Knox et al., 2015; Hemes et al., 2019). However, with rewetting, intensive agricultural production is in many cases not possible anymore. Hence, there is a trade-off between environmental goals and agricultural production demands that creates challenges to implementing peatland restoration (Ferré et al., 2019). Therefore, peatland management strategies, which could not only sustain the productive use of organic soil but also counterbalance soil subsidence and reduce N₂O emission, are urgently needed. It has been reported that artificial mineral soil coverage with thicknesses of 0.2–0.5 m is becoming an increasingly used practice in Switzerland and other European countries (Schindler and Müller, 2001; Ferré et al., 2019). Mineral soil coverage may have two main impacts on N and C transformation and N₂O emissions. First, it changes the topsoil properties of drained organic soil and influences substrate availability for N₂O production. As the soil depth from which emitted N₂O originates is only 0.7–2.8 cm, the topsoil properties are particularly relevant for N₂O emission (Neftel et al., 2000). After mineral soil coverage, the topsoil contains much less organic matter than the degrading peat. With this, carbon and nitrogen availability for denitrification might become limiting, thereby also influencing

TABLE 1 | Surface (0–10 cm) soil properties of drained organic soil with (Cov) and without (Ref) mineral soil coverage (*n* = 11).

Parameter	Cov	Ref
Bulk density (g cm ⁻³) ^a	1.1 ± 0.04	0.5 ± 0.01
pH	7.3	5.2
Sand (%) ^a	31.8	0.6
Silt (%) ^a	52.3	67.3
Clay (%) ^a	15.9	32.1
Total pore volume (%) ^a	58.4 ± 1.5	75.1 ± 0.5
Field capacity (%) ^a	51.4 ± 0.9	57.9 ± 0.6
Total N (%)	0.30 ± 0.03	1.46 ± 0.04
SOC (%)	3.57 ± 0.52	17.68 ± 0.47
C to N ratio	11.68 ± 1.15	12.12 ± 0.16
NH ₄ ⁺ (N mg kg ⁻¹ dry soil) ^b	2.62 ± 0.96	37.33 ± 12.07
NO ₃ ⁻ (N mg kg ⁻¹ dry soil) ^b	2.81 ± 1.21	5.16 ± 1.13

^aMeasured at depth of 3–8 cm, *n* = 12.

^b*n* = 8.

soil N₂O production (Stehfest and Bouwman, 2006; Flechard et al., 2007). Second, mineral soil coverage alters soil hydraulic properties and soil aeration due to the changing pore size distribution. Soil moisture and concomitantly the amount of oxygen are important regulators for microbial activity, thus affecting nitrification, denitrification, and subsequent N loss as N₂O (Davidson et al., 2000).

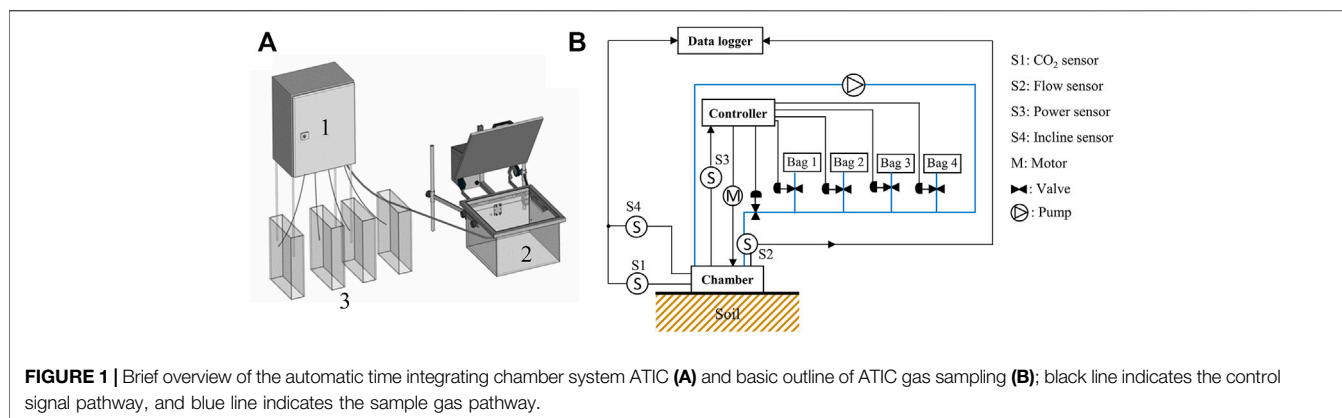
In Switzerland, peatlands covered an area of ca. 1,000–1,500 km² in preindustrial times. Today, most of the former organic soils are already lost, with only ~280 km² left. Ninety percent of the remaining organic soils are still drained for agriculture (Wüst-Galley et al., 2020) and continuously contribute to the national economic values of agriculture output. It is estimated that these soils emit around 1.2–7.9 kg N₂O-N ha⁻¹ yr⁻¹ (Leifeld, 2018), corresponding to an annual N₂O emission of c. 65 kt CO₂-eq, or ~10% of the national GHG emissions from drained organic soil (FOEN, 2021). However, hitherto neither N₂O flux measurements from organic soil do exist for Switzerland nor are experimental data available to quantify the impact of mineral soil coverage on N₂O emissions from drained peatland.

In this study, we utilized an automatic time integrating chamber system (ATIC) to determine the N₂O emission from long-term intensively managed temperate drained peatland with (Cov) and without (Ref) mineral soil coverage. Our specific objectives were to 1) quantify the N₂O emission from a drained nutrient-rich managed peat meadow in the Swiss Rhine valley and 2) explore the effect of mineral soil coverage on N₂O fluxes from this soil.

2 MATERIAL AND METHODS

2.1 Study Site

The measurements were carried out in the Swiss Rhine Valley, at the site Rütli (47°17' N, 9°32' E), a drained fen with a peat thickness of ~10 m. The site has a cool temperate moist climate with a mean annual precipitation of 1,297 mm and a mean annual temperature of 10.1°C (1981–2010, <https://www.meteoswiss>).



admin.ch). Drainage with ditches commenced before 1890 (<https://map.geo.admin.ch>). An integral drainage system with drainage pipes (depth 1 m, distance between pipes 14 m) and a pump was built in 1973; at the same time, the site was used as pasture until 2013, and since then as an intensively managed meadow with mineral and slurry fertilization and 5–6 grass cuts per year. In 2006–2007, one part of the field (1.7 ha) was covered with mineral soil material (thickness around 40 cm, see details in **Table 1**) to improve the trafficability and agriculture usability by raising the soil surface and counterbalancing peat subsidence. We established our field experiment at this mineral soil coverage site (Cov) and used the adjacent drained organic soil without mineral soil coverage as the reference (Ref, see details in **Supplementary Figure S1**). Both sites have identical farming practices and similar vegetation. Dominant grass species are *Lolium perenne*, *Alopecurus pratensis*, *Festuca arundinacea*, *Trifolium spec.*, and *Festuca pratensis*. The atmospheric N deposition at the study site as estimated for 2015 is 20–30 kg N ha⁻¹ yr⁻¹ (Rihm and Künzle, 2019).

2.2 N₂O Flux Measurements

2.2.1 Automatic Time Integrating Chamber System

The ATIC system used here was developed based on the automatic chamber system design introduced by Flechard et al. (2005), and the air sampling follows the system introduced by Ambus et al. (2010). The ATIC is operated as a non-steady-state flow-through chamber with a main loop that recirculates the headspace chamber air (**Figure 1**). The lid of the chamber closes automatically for 15 min. During this period, four headspace gas samples are collected (at 3.50, 7.25, 11.50, and 14.25 min after chamber closure) for 15 s and flushed into four different foil gas bags through a valve manifold. The use of the ATIC system allows flux measurements at relatively high frequency (like for online automatic chamber systems) but reduces the frequency of gas analysis and avoids the use of online trace gas analysis, which lowers the cost and energy consumption in the field. The ATIC runs with a battery (12 V) or power line, and the latter is used in our experiment. It consists of three parts: 1) a stainless steel chamber (L = l = 300 mm, H = 220 mm) with a pump (Thomas, Germany), CO₂ sensor (Senseair, Sweden), flow sensor (McMillan, New York

City, NY, United States), lid inclinometer sensor (DIS Sensors, Netherland), and motor connected with the lid of the chamber through pulley and rope (**Figure 1A**, unit 2); 2) an associated controller system, including the main control module (Siemens, Germany), and the data logger (Onset, MA, United States) for the sensors attached with the chamber (**Figure 1A**, unit 1); and 3) 4 replaceable foil gas bags (Supelco, Germany; **Figure 1A**, unit 3). The controlling system opens and closes the chamber lid through the motor. Each chamber was placed on a PVC frame, inserted 5 cm into the soil. Flexible silicone attached below the chamber and the foam sealing above the chamber was used to achieve gas tightness of the chamber.

2.2.2 N₂O Sample Accumulation and Analysis

N₂O fluxes were measured quasi-continuously for two entire years from 28 February 2019 to 02 March 2021. Here, we designate the first sampling year period (from 28 February 2019 to 28 February 2020) as the first year and the second sampling year period (from 28 February 2020 to 02 March 2021) as the second year. In the study site, the ATIC systems (four on Cov, four on Ref) were installed on 13 February 2019 for testing. On 28 February 2019, eight ATIC systems (four on Cov and four on Ref) started to collect gas samples with a frequency (time between measurement cycles) of 3–9 h per individual chamber, differing between growing season and non-growing season. Here, we define a measurement cycle as a lid closing phase of 15 min with sequential gas sampling into each of the four foil gas bags.

The bags were filled at 3.50, 7.25, 11.50, and 14.25 min after chamber closure, respectively, and the gas samples from individual cycles were accumulated in these four foil gas bags. The final bag samples represented an average over a time period of 3–14 days (hereafter referred to as “sampling period”), depending on the sampling frequency and the total number of measurement cycles. Usually, gas samples accumulated in the bags over 30–40 cycles, which was limited by the volume of the foil gas bag (10 L) and the flow rate of the pump (1 L min⁻¹). After the sampling period, the foil gas bags were replaced with empty ones, and the filled gas bags were transferred to the lab to determine their gas concentration using the gas analyzer (G2308, Picarro, Santa Clara, CA, United States). Overall, each

ATIC system was working for ~3,200 cycles during the two entire years. The foil gas bags have been tested and proven to be suitable for long-term storage of N₂O near ambient concentrations in air (**Supplementary Figure S2**).

2.3 N₂O Flux Calculation

For static (non-steady-state) chamber measurement, the increase in headspace gas concentration is widely thought to be linear during a short closure time (Charteris et al., 2020). The analysis of the gas bags as described in the previous section resulted in four average concentrations, $\bar{C}_1 \dots \bar{C}_4$, for each chamber and sampling period. Calculating a linear regression of the four concentrations against their sampling times (3.50, 7.25, 11.50, and 14.25 min after chamber closure) yielded the regression slope $\partial\bar{C}/\partial t$ (mg m⁻³ min⁻¹) from which the average flux of the sampling period was derived as:

$$F = \frac{V}{A} \times \frac{\partial\bar{C}}{\partial t}, \quad (1)$$

where V and A are the volume (m³) and the covered area (m²) of the static chamber, 0.02 m³ and 0.09 m², respectively. Since each average bag concentration \bar{C}_a is the arithmetic average of the respective concentrations in each cycle ($C_{a,b}$), where a ($a = 1, 2, 3, 4$) is the number of bags and b is the number of cycles, the average slope $\partial\bar{C}/\partial t$ also represents the average of the individual concentration increases of each measurement cycle ($\partial C_b/\partial t$) in the sampling period. Therefore, F (**Eq. 1**) represents the average gas flux of each sampling period.

The multiplication of gas fluxes during each sampling period F (mg N m⁻² day⁻¹) and the duration of each sampling period T (days) yielded the cumulative gas fluxes of each sampling period. Finally, the annual cumulative N₂O fluxes (F_a , kg N ha⁻¹) were calculated from the cumulative gas fluxes of each sampling period as given below:

$$F_a = \sum_{i=1}^{i=n} F_i * T_i, \quad (2)$$

where F_i is the N₂O emission (mg N m⁻² day⁻¹) from sampling period i , and T_i is the duration of each sampling period i (days).

N₂O fluxes resulted from fertilization induced N₂O peaks (F-peak) and background N₂O emissions. The comparison of N₂O emissions before and after a fertilization event allowed for the detection and quantification of F-peak N₂O emissions. Quantifying background N₂O emissions after fertilization event is challenging, and here, we use mean N₂O emissions one week before fertilization to represent the background N₂O emissions during the fertilization event and for further analysis of the F-peaks. Only when the observed N₂O emissions during a fertilization event were higher than the background N₂O emissions, we consider this as F-peak induced by the fertilization event.

2.4 Data Quality Control and Gap Filling

2.4.1 Data Quality Control

The accuracy of the ATIC system was accessed by the CO₂ and inclinometer sensors inside the chamber. The measurement of

the real-time headspace chamber CO₂ concentration and the incline angle between the lid and chamber allowed us to detect any operational chamber problem (e.g., leakage and power failure). The CO₂ fluxes during each chamber closure time were evaluated by linear regression, and an overall $R^2 \geq 0.9$ was taken as an indicator for a fully functional ATIC within the sampling period. With the comparison between the average CO₂ fluxes during each chamber closure time and the CO₂ fluxes from the ATIC system within each sampling period, we determined whether the gas fluxes from the ATIC system represented the average gas fluxes within the sampling period (**Supplementary Figure S3**). N₂O fluxes calculated from the concentration gradient from the four foil gasbags were selected for post-processing after fulfilling certain quality criteria. First, R^2 of CO₂ fluxes calculated from the regression lines of the four bags had to exceed 0.9, indicating that within the sampling days, the ATIC worked properly. $R^2 \leq 0.9$ indicated a failure of gas sampling within the sampling days, which led to a rejection of the N₂O flux data. Second, $R^2 > 0.9$ of the N₂O regression lines was used as critical to accept the data for further analysis. However, low fluxes (± 0.5 mg N m⁻² day⁻¹, calculated based on the detection limit of the Picarro) were accepted regardless of R^2 . With low fluxes, the random error of the measurement could be larger than the N₂O concentration difference between different sampling points, which could result in low R^2 , and therefore, rejection of the N₂O emission based on low R^2 would lead to an underestimation of the overall fluxes. After two years of continuous field observation, the N₂O data could cover ~86% of the sampling days, that is, a data gap of ~14%.

2.4.2 Gap Filling

For any missing N₂O emissions outside the fertilization event (background N₂O emissions), that is, values missing owing to a failure of ATIC systems or a rejection of data, a look-up table approach with two parameters (soil moisture and soil temperature) was used to fit the missing values ($RMSE = 0.62$ mg N m⁻² day⁻¹, $R^2 = 0.60$), and tested by the available background N₂O values through cross-validation. For each chamber, background N₂O emissions were divided into 16 classes based on soil moisture (0–25th percentile, > 25th percentile–median, > median–75th percentile, and > 75th percentile), and soil temperature (0–25th percentile, > 25th percentile–median, > median–75th percentile, and > 75th percentile). With the assumption that without extra fertilizer input background N₂O should respond similar to similar soil temperature and moisture conditions at each site, the mean N₂O fluxes from each class were used to fit the missing value under the same soil temperature and moisture condition. To check the sensitivity of the N₂O gap-filling method for the background fluxes, two other methods were compared with the look-up table approach: 1) linear interpolation ($RMSE = 0.65$ mg N m⁻² day⁻¹, $R^2 = 0.51$) to bridge the missing values and 2) taking mean values from the properly operating chambers for each site ($RMSE = 1.3$ mg N m⁻² day⁻¹, $R^2 = 0.36$). For an N₂O gap caused by a power failure during the fertilization event on 30 August 2019 (site Ref), data were linearly interpolated to fill the data gap. For the failure of individual chambers ($n = 6$) during fertilization

events, mean values from the properly operating chambers at each site were used to fill the data gap.

2.5 Additional Measurements

2.5.1 Environmental Variables

The air temperature was measured using a Vaisala Weather Transmitter (WXT520, Finland) and continuously logged every 10 min on a CR1000 data logger (Campbell Scientific, United Kingdom). Rainfall data and missing air temperature (27 December 2020 to 2 February 2021) were filled with data from a nearby meteorological station operated by MeteoSwiss (<https://www.meteoswiss.admin.ch>). Soil temperature and soil moisture (GS3 and 5 TE decagon devices, NE Hopkins Court, United States) were continuously recorded half-hourly at a depth of 5 cm for both Cov ($n = 3$) and Ref ($n = 3$). On 4 December 2019, 24 additional soil temperature sensors (UA-001-64 devices, Onset, MA, United States) were installed near each chamber at three depths (0, 2.5, and 5 cm) for recording surface soil temperature in winter. These sensors were taken out on 21 April 2020 for reading out the data, and the same process was followed for winter 2020/2021. Close to the chambers, the soil volumetric water contents at -5 cm depth were consistently recorded every 10 min with soil moisture sensor (EC-5, decagon devices, NE Hopkins Court, United States). Missing soil temperature data—due to a failure of a data logger between November to December 2019 and April to May 2020 (site Cov)—were fitted using linear regression between temperatures of the two sites with a similar temperature range ($RMSE = 0.07^{\circ}\text{C}$, $R^2 = 0.98$).

2.5.2 Soil Properties and Fertilizer Nutrient

To determine the soil pore volume, on 12 April 2019, 72 undisturbed cylindrical soil samples (100 cm^{-3}) were collected at three depths (3–8, 18–23, and 58–63 cm) with 12 replications at each site and transferred to the laboratory. In the laboratory, different pore diameters were measured following the approach by Keller et al. (2019). For this, samples were saturated from below and then drained to soil matric potentials of -30 , -60 , -100 , -300 , and $-1,500$ kPa.

Air porosity was calculated based on the difference between volumetric water content (VWC) and total pore volume. The relative gas diffusion coefficient (D_p/D_0) was calculated based on air-filled porosity by following the approach by Keller et al. (2019). A D_p/D_0 of 0.02 has been suggested as the critical threshold for adequate soil aeration, and the D_p/D_0 value lower than 0.02 indicates insufficient soil aeration (Schjønning et al., 2003). The water-filled pore space was determined by the ratio of volumetric water content and total pore volume, and field capacity was determined by water retention at -30 kPa. Here, we used the threshold of 80% of the field capacity for each site to roughly distinguish dry and wet conditions separately for Cov and Ref. Soil moisture of below 80% of the field capacity was designated as dry, and $>80\%$ of the field capacity as wet.

For soil organic carbon (C) and total nitrogen (N) content measurement, 22 soil samples were taken in 2018, with 11 replications at each site. Soil samples were dried at 105°C for

72 h, ground using mortar and pestle, and then milled in a ball mill (Retsch, MM 400, Germany) at $25\text{-rotation s}^{-1}$ for 3 min. Samples containing carbonate (soil surface from Cov) were fumigated with hydrochloric acid overnight in a desiccator before being analyzed by elemental analysis (Hekatech, Germany). For soil pH, soil (unground) was suspended 10 g in 0.01 M calcium chloride (CaCl_2), shaken at $160\text{ cycles min}^{-1}$ for 15 min, and left overnight before the soil pH was measured with a flat surface electrode (pH3310, WTW, Germany). For ammonium and nitrate measurements, 16 soil samples were taken in July 2021, with eight replications at each site. Soil N was extracted from 20 g field-moist soil with 0.01 M CaCl_2 solution and filtered. The filtrate was analyzed by segmented flow injection analysis (Skalar Analytical B.V., Breda, Netherlands). The C and N content in the slurry was determined in a central laboratory (Labor für Boden und Umweltanalytik, Eric Schweizer AG, Thun, Switzerland). For details about N application rate and frequency, see Table 2).

2.6 Data Analysis

Plots and statistical analysis were performed using open-source software R (version 3.6.0, The R Project, 2014). N₂O emissions as measured by the ATIC systems were calculated based on linear regression in R. Environmental parameters including soil temperature, soil moisture, air-filled porosity, and D_p/D_0 were calculated and plotted as daily means. A multiple linear regression (MLR) model with unstandardized explanatory variables was used to evaluate the drivers for the F-peak and daily background N₂O emissions, with soil temperature, water-filled pore space, and nitrogen (N) input as explanatory variables. For each of those variables, its statistical significance to the MLR model was chosen as $p < 0.05$. The adjusted coefficient of determination (R^2_{adj}) is then given by the number of driving variables and the sample size, and is used to describe the explained variation of the dependent variable. For the daily background N₂O emissions, the minimum N₂O flux plus one (which was determined by the minimum observed N₂O emission data) was added to N₂O fluxes separately for the two sites and log-transformed before being applied to the MLR model. The difference in soil temperature, soil moisture, air-filled porosity, daily N₂O emission, annual N₂O emission, daily N₂O emission from fertilization events (daily F-peak N₂O), fertilization-induced N₂O peaks, daily background N₂O emission, and cumulative background N₂O emission were analyzed for statistical difference between Cov and Ref by using a t -test. An error probability of $p < 0.05$ was chosen. Results are always reported as mean ± 1 standard error (se).

For the annual N₂O emission from Cov and Ref, we calculated the standard error based on the spatial variability among the four ATIC systems for both sites. The annual cumulative se of each N₂O flux calculation by linear regression within each chamber contributed only 0.1% to the se derived from the spatial variability of the four replicates. Therefore, we believe that the se derived from spatial variability covers the overall se inherent to our N₂O flux calculations.

TABLE 2 | Fertilization event-induced nitrous oxides (N₂O) fluxes (mean ± se, n = 4) and associated environmental parameters, soil temperature (T_{soil}), and water-filled pore space (WFPS) from drained organic soil with (Cov) and without (Ref) mineral soil coverage.

Date	Fertilization (kg N ha ⁻¹)	F-peak N ₂ O flux (kg N ha ⁻¹)		Fraction of N loss* (%)		T _{soil} (°C)		WFPS (%)	
		Cov	Ref	Cov	Ref	Cov	Ref	Cov	Ref
28 March 19 ^a	87	0	0	0	0	8.0	8.1	53.7	53.6
03 June 19 ^b	32	0.01 ± 0.009	0.07 ± 0.02	0.03 ± 0.02	0.22 ± 0.04	18.6	18.8	57.8	65.6
06 August 19 ^a	85	2.01 ± 0.32	25.50 ± 2.15	2.37 ± 0.38	30.04 ± 2.53	20.8	20.3	67.6	69.0
24 March 20 ^a	62	0	0	0	0	5.8	5.5	73.3	73.4
27 April 20 ^a	65	0.16 ± 0.05	0.77 ± 0.31	0.25 ± 0.07	1.18 ± 0.47	15.0	14.8	67.6	69.7
02 June 20 ^b	26	0.13 ± 0.008	0.70 ± 0.23	0.50 ± 0.03	2.69 ± 0.88	17.8	17.7	67.1	69.4
07 July 20 ^b	26	0.28 ± 0.07	1.43 ± 0.56	1.08 ± 0.27	5.50 ± 2.16	21.4	20.9	66.9	70.3
10 September 20 ^a	74	0.003 ± 0.005	0.62 ± 0.16	0.004 ± 0.007	0.84 ± 0.21	20.6	19.8	61.1	62.9

*Equivalent fraction of fertilization induced N₂O emission and the fertilizer N input, mean ± SE (n = 4).

^aNitrogen (N) inputs as slurry.

^bNitrogen (N) inputs as synthetic fertilizer.

3 RESULT

3.1 Environmental Conditions

The two sampling years had a mean annual air temperature of 10.7°C (**Figure 2A**) and annual precipitation of 1,535 mm. The latter was higher in the first (1,690 mm) than in the second year (1,380 mm, **Figure 2B**). The two years and two sites had similar daily mean soil temperature on average. At both sites, 5 cm soil temperature was continuously above 0°C during the two sampling years despite frequent winter frost (**Figure 2A**). In the second year, spring and summer were moister with ~10.9 and ~11.4% higher ($p < 0.01$) soil water-filled pore space (WFPS) during March to June and June to August, respectively, than in the first year. Soil WFPS was not different between sites but more variable for Cov (30.8–91.6%) than for Ref (24.2–76.4%, **Figure 2B**). During spring and summer of 2019, air-filled porosity was higher ($p < 0.05$) than that in 2020 by ~3.9 and ~5.4%. Air-filled porosity was almost continuously higher ($p < 0.01$) at Ref than at Cov (**Figure 2C**). Consequently, the relative gas diffusion coefficient of Ref exceeded that of Cov ($p < 0.01$). At Cov, the relative gas diffusion coefficient was lower than the critical threshold for adequate soil aeration (0.02) at 172 days, whereas it never passed the critical threshold at Ref (**Figure 2D**).

3.2 N₂O Emissions

The N₂O emissions integrated over two years of continuous field measurement from Ref exceeded that of Cov by a factor of 9 (**Figure 3**). Daily N₂O emissions showed a larger variability during the first year, ranging from -0.02 to 242.01 mg N m⁻² day⁻¹ for Ref, and from -0.04 to 22.08 mg N m⁻² day⁻¹ for Cov. During the second year, daily N₂O emission ranged from -0.04 to 18.41 mg N m⁻² day⁻¹ for Ref and from -0.04 to 2.80 mg N m⁻² day⁻¹ for Cov (**Figure 3**). At Ref, the average daily N₂O emissions during the first year was 8.98 ± 1.03 mg N m⁻² day⁻¹, which was higher ($p < 0.01$) than that of Cov (0.86 ± 0.10 mg N m⁻² day⁻¹, see **Figure 4C**).

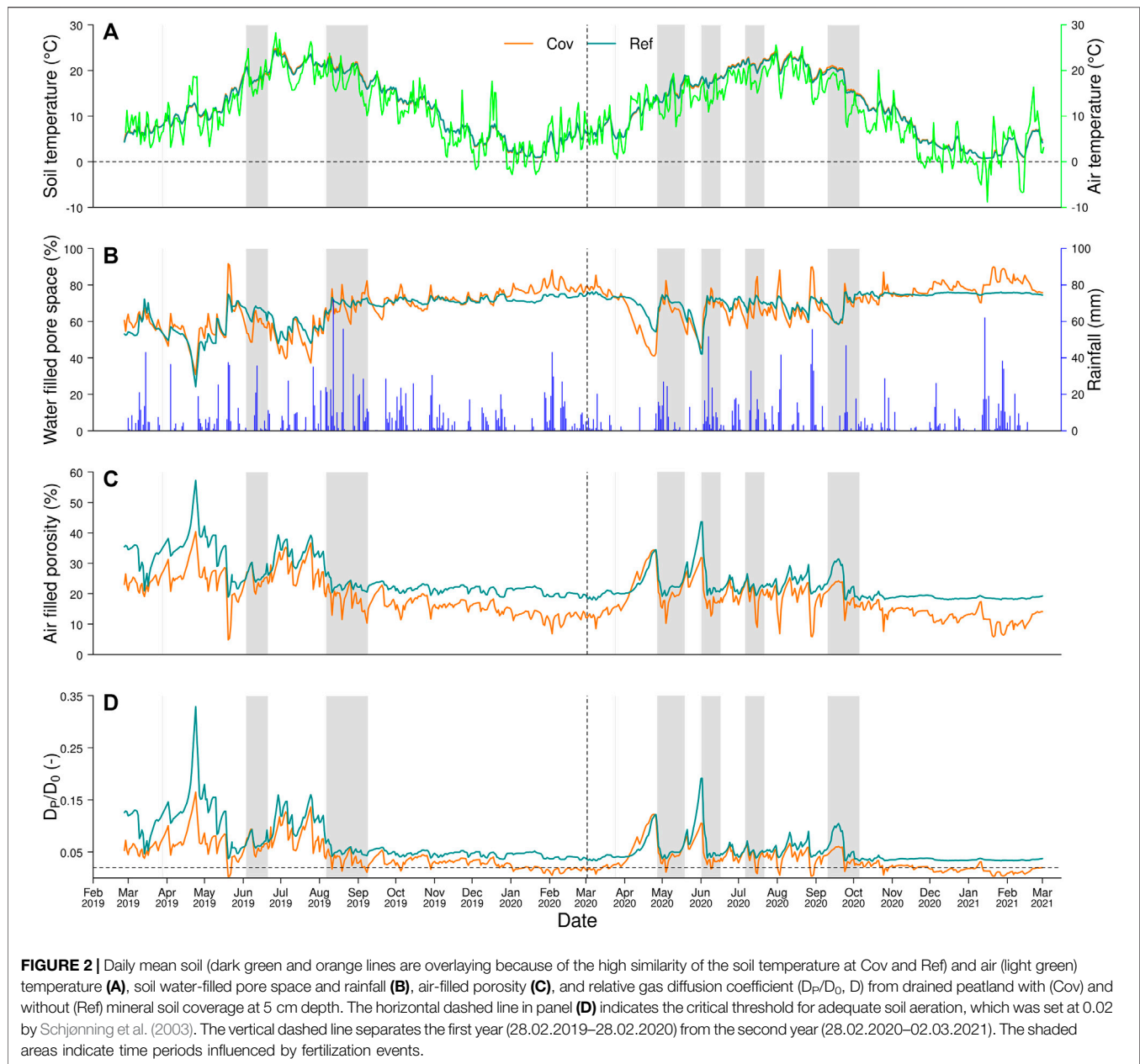
Overall, N₂O emissions differed largely between the two sites and the two years. At Ref, emissions were ~4 times higher during the first year than during the second year. At Cov, the first year

emissions were ~2 times higher than the second year ones. The annual N₂O fluxes for the two years were different for both sites, but the N₂O emissions from Ref were still clearly higher ($p < 0.01$) than those from Cov. In the first year, the cumulative annual N₂O flux from Ref was 32.71 ± 3.87 kg N ha⁻¹ yr⁻¹, around 11 times higher than Cov (3.18 ± 0.35 kg N ha⁻¹ yr⁻¹; **Figure 4A**). In the second year, the annual N₂O fluxes from Ref was 8.28 ± 1.77 kg N ha⁻¹ yr⁻¹ (**Figure 4B**), which was around six times higher than Cov (1.33 ± 0.23 kg N ha⁻¹ yr⁻¹). The difference of N₂O emissions between the sites was not only related to higher ($p < 0.01$) fertilization-induced peak N₂O emissions from Ref (42.48 ± 3.34 mg N m⁻² day⁻¹) than Cov (3.41 ± 0.54 mg N m⁻² day⁻¹) but also driven by higher ($p < 0.05$) background N₂O emissions from Ref (1.63 ± 0.46 mg N m⁻² day⁻¹) than Cov (0.27 ± 0.04 mg N m⁻² day⁻¹, see **Figure 4C**). A similar pattern was seen in the second year (**Figure 4D**).

3.3 Main Driving Factors of N₂O Emissions

3.3.1 Fertilization Effect

At both sites, high N₂O emission peaks were primarily triggered by fertilization events (F-peak) and lasted for 2–3 weeks before returning to background N₂O emissions (**Figure 3**). There were eight fertilization events during the experimental period, but we only observed six F-peaks during summer and autumn when the soil temperature was high (**Table 2**). To further explore the influence of N input on N₂O emissions, we defined a corresponding fraction of N loss as the ratio of the N₂O emissions during each F-peak and the corresponding fertilizer N input. We found the fraction of N loss to be higher at Ref than at Cov ($p < 0.01$) for each of the six individual F-peaks. In the first year, F-peaks contributed ~78% to the annual N₂O emissions at Ref, corresponding to 25.56 ± 2.15 kg N ha⁻¹. At Cov, F-peaks contributed ~64% to the annual N₂O emissions, corresponding to 2.02 ± 0.32 kg N ha⁻¹ (**Figure 4A**). For the second year, at both sites, F-peak fluxes only contributed ~43% to the annual N₂O emissions, corresponding to 3.51 ± 0.84 kg N ha⁻¹ for Ref and 0.57 ± 0.11 kg N ha⁻¹ for Cov (**Figure 4B**). It needs to be noted that during the fertilizer event in August 2019, we observed a relatively high peak at both sites (**Figure 3**), which extended over

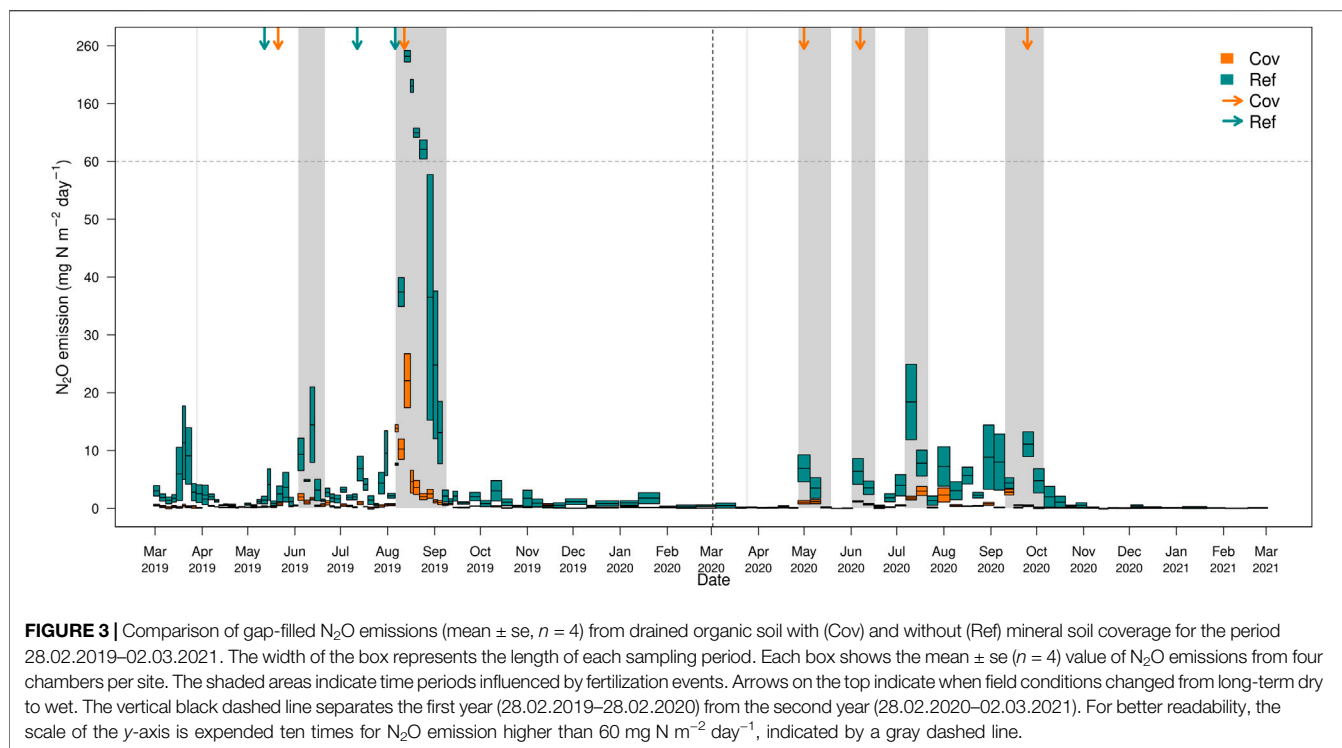


25 days (8 sampling periods). The N₂O emissions from this high peak contributed ~78% to the annual N₂O emissions to Ref and ~64% to Cov.

3.3.2 Environmental Parameters

In order to identify the main driving factors for N₂O emissions, regression analyses were applied separately on fertilization-induced and background N₂O emissions. For fertilization-induced N₂O emissions, the regression analysis was performed on each individual fertilization-induced F-peak. We found that 50 to 60% of the variation in F-peak N₂O emissions could be explained by the multiple linear regression model with soil temperature, soil water-filled pore space, and amount of N input as explanatory variables (Table 3). At both sites, the

variability of F-peak emission was mainly driven by soil temperature and N inputs ($p < 0.05$; $p < 0.01$), and the two parameters were positive drivers for F-peak N₂O emissions. In addition, the average WFPS during the fertilization events also contributed significantly to the variability of the F-peak N₂O emissions at both sites. For background N₂O emissions, the variation in N₂O emissions explained by the MLR model was low with R^2 of 0.10 (Cov) and 0.16 (Ref). The impact of the two potentially driving parameters soil temperature and soil WFPS differed between Cov and Ref. Overall, soil temperature was a significant driver for background N₂O emissions at both sites ($p < 0.01$), but the effect of soil WFPS on background N₂O emissions was not significant (Table 3). A threshold of 80% of the field capacity was used to define dry and wet conditions in the field. At



Ref, soil WFPS was a positive driver for background N₂O emissions during dry conditions in the field, whereas it was negative under wet conditions ($p < 0.01$). At Cov, soil WFPS only exerted limited influence on background fluxes.

4 DISCUSSION

4.1 Magnitude of N₂O Fluxes From the Two Sites

Our continuous two years of field N₂O observation showed that the drained nutrient-rich fen (Ref) emitted 20.5 ± 2.7 kg N ha⁻¹ yr⁻¹. This was substantially higher than the IPCC default value and its 95% confidence interval, 8.2 (4.9–11) kg N ha⁻¹ yr⁻¹ (IPCC, 2014). Moreover, the study site also emitted substantially more N₂O than 25 measured fen peats in Germany (average 2.9 ± 2.7 kg N ha⁻¹ yr⁻¹; Tiemeyer et al., 2016), and also more than the average from drained grassland organic soils from 217 annual budgets across Europe (5.8 ± 10.3 kg N ha⁻¹ yr⁻¹; Leppelt et al., 2014). However, the annual N₂O emissions from the study site were lower than the N₂O emissions from drained fens with high organic carbon in Slovenia (37.1 ± 0.2 kg N ha⁻¹ yr⁻¹; Danevčič et al., 2010). In our opinion, these differences in the N₂O emissions from drained fens between our site and the bulk of measurements from temperate grasslands are mainly driven by climate conditions and the amount of fertilizer input. Compared with the overall peatland distribution across Europe (Tanneberger et al., 2017), our site and the Slovenian site (Danevčič et al., 2010) are situated in regions with relatively high soil temperatures, particularly during summer. This may foster higher N₂O emissions, owing to the

normally positive correlation between soil temperature and N₂O emission that we found, in line with previous studies (Marushchak et al., 2011; Parn et al., 2018). Regarding fertilizer input, our site received c. 230 kg N ha⁻¹ yr⁻¹, which is much above the average rate of ~44 kg N ha⁻¹ yr⁻¹ for drained grassland organic soils across Europe (Leppelt et al., 2014), and ~52 kg N ha⁻¹ yr⁻¹ of drained fens managed as grassland in Germany (Tiemeyer et al., 2016). Moreover, for some of the study sites mentioned by Tiemeyer et al. (2016), where fertilizer input was higher than 300 kg N ha⁻¹ yr⁻¹, these authors also reported higher N₂O emissions of 6.4–27.2 kg N ha⁻¹ yr⁻¹.

With mineral soil coverage, the N₂O emissions were strongly reduced (2.3 ± 0.4 kg N ha⁻¹ yr⁻¹) and also lower than the IPCC emission factor for managed deeply drained nutrient-rich grassland on organic soil (8.2 kg N ha⁻¹ yr⁻¹; IPCC, 2014). It is not possible to compare the N₂O emission from Cov with former studies, because no N₂O emission data from drained peatland with artificial mineral soil coverage exist up to date. The observed N₂O emissions from Cov were in the range of N₂O emissions from mineral grassland soils in Switzerland. These have been reported to be 1.0–2.6 kg N ha⁻¹ yr⁻¹ N₂O-N from an intensively used grassland in the temperate Swiss Central Plateau with a fertilization rate of ~200 kg N yr⁻¹ (Flechard et al., 2005); 2.2–7.4 kg N ha⁻¹ yr⁻¹ from another intensively used grassland in the Swiss Central Plateau during 2010–2011 and 2013–2014 with extra total N inputs of ~350 kg N yr⁻¹ (Merbold et al., 2021); and 3.9–5.9 kg N ha⁻¹ yr⁻¹ from an intensively used grassland in the Swiss Plateau during 2013–2016 with extra total N inputs of ~270 kg N yr⁻¹ (Fuchs et al., 2020). Based on IPCC (2019), a fertilizer N input of c. 45 kg N ha⁻¹ yr⁻¹ mineral and c. 185 kg N ha⁻¹ yr⁻¹ organic fertilizer nitrogen (N) as in our

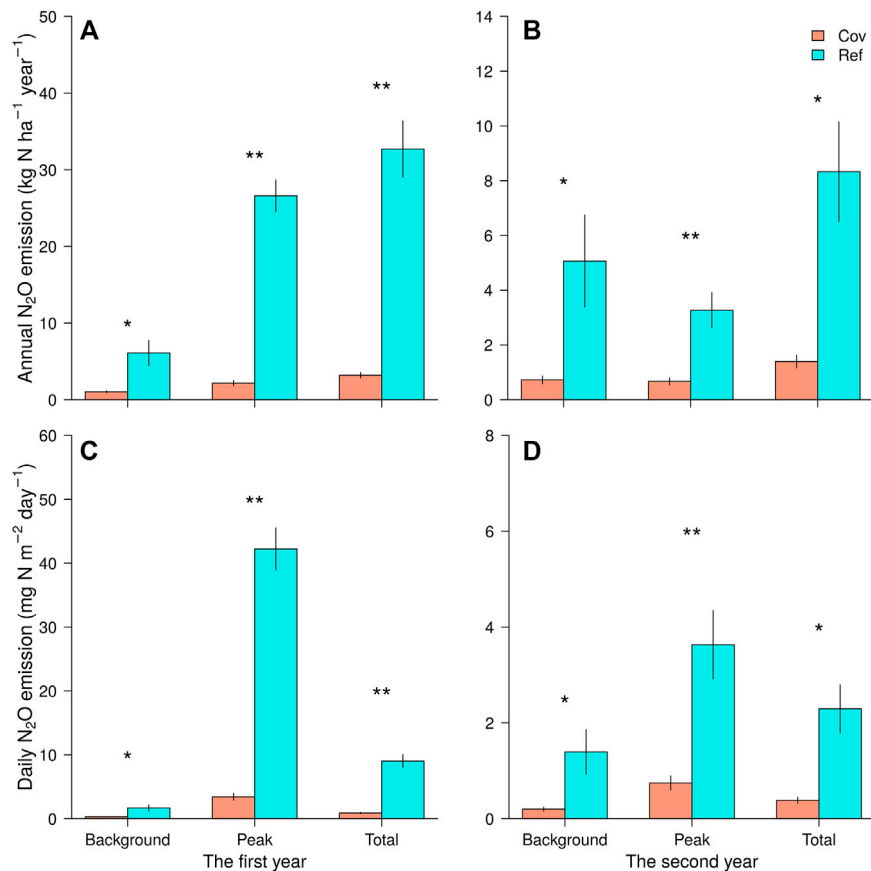


FIGURE 4 | Cumulative N₂O emissions (mean ± se, $n = 4$) and contribution of the emission types to the overall field N₂O emission from drained organic soil with (Cov) and without (Ref) mineral soil coverage during the first year (A) and the second year (B); and average daily N₂O emission (mean ± se, $n = 4$) for two emission types during the first year (C) and the second year (D). Significant differences between the two sites are indicated with asterisks (**** $p < 0.01$, *** $p < 0.05$).

TABLE 3 | Regression analysis using log-transformed background N₂O fluxes, and fertilization-induced N₂O fluxes from each chamber as the dependent variable and soil temperature (T_{soil}), water-filled pore space (WFPS), and nitrogen input (N input) as explanatory variables.

Site	Parameters	R ² (R ² adj)	a (T_{soil})	b (WFPS)	c (N input)	d (intercept)
Log-transferred background N ₂ O fluxes						
Cov ($n = 392$)	Overall	0.11 (0.10)**	0.007**	0.0006	—	-0.17**
	WFPS ≥80% field capacity	0.28 (0.28)**	0.015**	0.01**	—	-1.04**
	WFPS <80% field capacity	0.03 (0.02) *	0.004**	0.001	—	-0.15*
Ref ($n = 392$)	Overall	0.16 (0.15)**	0.02**	-0.003	—	0.19
	WFPS ≥80% field capacity	0.26 (0.25)**	0.019**	-0.022**	—	1.62**
	WFPS <80% field capacity	0.11 (0.09)**	0.007**	0.013**	—	-0.45*
Cumulated peak N ₂ O fluxes (kg N ha ⁻¹)						
Cov ($n = 48$)	N ₂ O fluxes	0.67 (0.60)**	0.11*	0.04**	0.02**	-6.32**
Ref ($n = 48$)	N ₂ O fluxes	0.61 (0.53)**	1.80*	0.69*	0.24**	-91.11**

In the analysis, the linear model $y = ax_1 + bx_2 + cx_3 + d$ was used for multiply linear regression. The error probability is indicated by asterisks (**** $p < 0.01$, *** $p < 0.05$).

study site would induce an N₂O emission of 0.8–2.9 kg N ha⁻¹ yr⁻¹, and the average rate measured in Cov is within the range. Therefore, it seems that with mineral soil coverage, the drained organic soil of our site behaves like mineral soil in terms of its N₂O release.

4.2 Drivers of N₂O Emissions and Effects of Mineral Soil Coverage

4.2.1 Drivers of N₂O Emissions for the Two Sites

In our study, soil temperature, soil water-filled pore space, and N input could explain more than half of the variance of

fertilization-induced N₂O emissions (F-peak; **Table 3**). Higher F-peaks were found with warm temperatures and lower with cold temperatures (**Table 2**), most likely due to the reduced soil microbial activity (Holtan-Hartwig and Bakken, 2002). The fertilizer N inputs and the high WFPS did not compensate for the effect of cold temperatures (**Table 2**), indicating that in our field, high N₂O peaks only occur if all the driving variables (soil temperature, soil water content, and N availability) are supporting high N₂O production. Previous research also highlighted that peak N₂O emissions were not observed if one driving factor was below thresholds for soil temperature and moisture (Holtan-Hartwig and Bakken, 2002; Meng et al., 2005). In turn, if these driving factors were above the threshold, a fertilization event will lead to very high N₂O emissions. In the first year, we observed a very high F-peak after fertilization in August, which contributed more than half to the annual N₂O emissions for both sites and even 78% for Ref. This led to a significantly higher annual N₂O release in the first year than in the second year. One explanation might be the time line of the dry summer period followed by a wetting event together with the fertilizer application (**Figure 3**). This interpretation is supported by a large body of former research works that after dry and wet cycles for both mineral soils and organic soils, a greater amount of N₂O is emitted from grassland owing to the enhanced availability of C and N as related to soil organic matter mineralization (Priemé and Christensen, 2001; Beare et al., 2009; Harrison-Kirk et al., 2013). The differences in fertilization-induced N₂O emissions under different soil temperatures and soil WFPS suggest that as one N₂O mitigation option for the study site, fertilizer application should be avoided in hot summer periods or during frequent precipitation.

4.2.2 Drivers of N₂O Reduction After Mineral Soil Coverage

Despite receiving the same amount of N input and having similar soil temperatures and WFPS, as well as the same agricultural management, Ref had much higher N₂O emissions after fertilization. The different N₂O releases after fertilization might be related to various mechanisms. First, exogenous N inputs might prime the mineralization of SOM, thereby influencing N₂O production differently in Cov and Ref. Priming effects are defined as short-term changes of SOM mineralization in response to external stimuli, for example, exogenous N addition, and they alter the subsequent N₂O production from SOM-N (Kuzakov et al., 2000; Daly and Hernandez-Ramirez, 2020; Thilakarathna and Hernandez-Ramirez, 2021). Priming may affect N₂O emissions positively or negatively, depending on soil moisture and SOM content (Roman-Perez and Hernandez-Ramirez, 2020). Former studies revealed positive N₂O priming effects to be associated with wetter soil conditions (WFPS >60%) and higher SOM content (Schleusner et al., 2018; Thilakarathna and Hernandez-Ramirez, 2021). In our study site, soil moisture for Cov and Ref were similar during the fertilization events (**Table 2**), but SOC content in surface soil of Ref was five times higher than that in surface soil of Cov (**Table 1**), which might have induced stronger priming by adding N, subsequently leading also to higher N₂O emissions for Ref (Perveen et al., 2019). For the background N₂O

emissions, soil temperature was still a significant driver at both sites, but the influence of the soil water-filled pore space was limited (**Table 3**). Moreover, the variance of background N₂O emissions explained by the MLR model with soil temperature and soil water content was low, indicating that for both sites, the influence of soil temperature and soil moisture on background N₂O emission was limited. In our study, background N₂O emissions were also significantly reduced ($p < 0.05$) with mineral soil coverage, indicating that the higher N₂O emission from Ref was not only directly related to fertilization but also to the properties of the surface soil itself, for example, soil pH and soil N availability. Surface soil properties are of particular relevance for the amount of N₂O release as it has been shown that the soil depth from which emitted N₂O originates is only 0.7–2.8 cm (Neffel et al., 2000).

Second, surface soil pH increased from 5.2 to 7.3 (**Table 1**) with mineral soil coverage in our study site. It has been reported that the net production of N₂O from denitrification is strongly dependent on soil pH (Nadeem et al., 2020); N₂O emissions are negatively correlated with soil pH in organic soil, due to the decreased N mineralization with increasing soil pH under aerobic conditions of peat (Chapin et al., 2003; Weslien et al., 2009) and the possible enhancement of the synthesis of functional N₂O reductase from denitrification (Liu et al., 2014), resulting in a higher share of N₂. Hence, the relatively high soil pH at Cov may have contributed to the lower background N₂O emissions.

Third, the two topsoils differed in soil N content and soil N availability (**Table 1**). Soil available N from SOM mineralization is considered to be the main source for background N₂O production (Lampe et al., 2006). Our study site revealed a carbon loss of 3,100–6,300 kg C ha⁻¹ yr⁻¹ from peat oxidation after drainage based on a former study using a radiocarbon approach to estimate the soil carbon loss (Wang et al., 2021). Considering the C to N ratios of ~25 (at a depth of 2 m) as representative for nitrogen stored in peat without fertilization, the study site has an N mineralization potential of 120–250 kg N ha⁻¹ yr⁻¹. This relatively high soil N supply at Ref, as also indicated by higher available soil N (**Table 1**), becomes available for microbial processing and consequently N₂O production. After mineral soil coverage with a thickness of ~40 cm, N release from peat mineralization of topsoil SOM as an N source for N₂O formation is no longer available. Instead, mineralization of SOM from the mineral soil coverage, whose soil N content and the corresponding soil available N are much lower (**Table 1**), becomes a major N source. The decreased surface soil N availability due to mineral soil coverage for nitrification and denitrification may then restrain the N₂O production (Senbayram et al., 2012). As one consequence for management, the high soil N supply in drained peatland suggests that the fertilization demand for organic grassland soils might be substantially lower than that for mineral grassland soils.

Fourth, although the organic soil at site Cov still has the potential to produce N₂O, the mineral soil coverage might have pushed the organic soil underneath into a deeper zone with higher soil moisture and lower oxygen availability as compared to the organic topsoil at site Ref. Higher soil moisture could influence the exchange of N₂O between the site of production and the aerated

pore space, thereby affecting the balance between N₂O production and consumption. With high soil moisture, a reduction of N₂O emission is expected owing to the higher consumption of N₂O when gas diffusion is slow (Kuang et al., 2019; Harris et al., 2021). Moreover, under strongly anaerobic conditions, N₂ as the end product of denitrification will be produced preferentially (Davidson et al., 2000). Thus, the amount of formed N₂O from the organic soil underneath might be reduced at site Cov *via* enhanced dissolution in soil water (Clough et al., 2006; Goldberg et al., 2008) or full denitrification before escaping into the atmosphere (Davidson et al., 2000). These effects are further pronounced by the lower gas diffusivity of the surface soil of Cov compared to Ref (Figure 2D). We suppose these effects in combination lead to lower N₂O emissions after mineral soil coverage.

4.3 Potential of N₂O Reduction by Mineral Soil Coverage

Based on two years of continuous field observation, the results from our study site showed that mineral soil coverage as a management option for organic soils induced a strong reduction of N₂O emissions from drained organic soil in the Swiss Rhine valley. In Switzerland, ~ 250 km² organic soils are still drained for agricultural production (Wüst-Galley et al., 2020), and N₂O release contributes by ~ 10% to the overall c. 650 kt CO₂ -eq yr⁻¹ GHG emissions from these soils (FOEN, 2021). Globally, c. 2.7 × 10⁵ km² peatlands are drained for agricultural (grassland and cropland) production, those areas are estimated to result in c. 1,046 Mt CO₂ -eq yr⁻¹ GHG emissions, and N₂O release contributes by ~ 24% to it (FAOSTAT, 2019; Evans et al., 2021). Rewetting has been suggested as key to reducing those GHG emissions from drained organic soils (Hemes et al., 2019; Günther et al., 2020; Ojanen and Minkkinen, 2020). However, in many areas, rewetting of all of those areas will be difficult to be achieved. First, for some countries, cultivation on drained organic soils is continuously making significant contributions to the economic development; therefore, rewetting of those areas might cause economic losses. Second, global demand for food and feed production and pressure on land is continuously increasing (FAO, 2017). These set barriers for full rewetting of drained agricultural organic soil despite the need for GHG reduction (Biancalani and Avagyan, 2014). Thus, in situations where full rewetting is not possible, mineral soil coverage might become a promising building block for GHG mitigation and, at the same time, counterbalance soil subsidence and maintain the productivity of drained organic soil.

5 CONCLUSION

Draining organic soil for intensive agricultural production induced N₂O emissions of 20.5 ± 2.7 kg N ha⁻¹ yr⁻¹ at our study site, which were reduced to 2.3 ± 0.4 kg N ha⁻¹ yr⁻¹ by mineral soil coverage. Most of the N₂O emissions were related to fertilization, and a single fertilization event under suitable soil temperature and soil moisture may contribute by more than half to the annual N₂O emissions in our study site, underpinning the need for high-frequency flux

measurements. Mineral soil coverage of drained organic soil could significantly reduce both fertilization-induced N₂O emissions and background N₂O emissions. The large potential of N₂O reduction after mineral soil coverage, which itself is a measure applied by farmers to counterbalance soil subsidence, provides an opportunity for not only reducing the environmental footprint of using drained organic soils but also for maintaining their agricultural productivity, and hence, farmers income. We are not aware of any management options apart from peatland restoration and rewetting that have the potential to substantially reduce N₂O emissions from organic soils. Mineral soil coverage of intensively used drained peatlands, which are not suitable for rewetting owing to soil conditions or socio-economic constraints, may therefore be a prospective management strategy for the sustained use of these soils. Our findings encourage further research on this measure, particularly for tropical conditions where drained peatlands are GHG hotspots and contribute the most to the overall emissions from managed organic soils (Dommain et al., 2018; Leifeld and Menichetti, 2018).

DATA AVAILABILITY STATEMENT

The original contributions presented in the study are included in the article/**Supplementary Material**; further inquiries can be directed to the corresponding author.

AUTHOR CONTRIBUTIONS

YW, SP, CA, and JL: conceived and designed the study. YW and MJ: collected and analyzed the samples. JL: managed the project. MJ: designed experimental instrument. YW: performed data analysis and drafted the original manuscript. SP, CA, MJ, and JL: edited the manuscript. All the authors read and approved the final manuscript.

FUNDING

The research was supported by funding received from the Swiss Federal Office for the Environment (contract number 06.0091. PZ/R261-2425), and the China Scholarship Council (NSCIS 201806350221).

ACKNOWLEDGMENTS

We acknowledge the help of Stefan Gloor, Robin Giger, Urs Zihlmann, and Marlies Sommer at Agroscope during field sampling and lab analysis. We are thankful for many insightful discussions with Christof Ammann and Karl Voglmeier at Agroscope. We thank Bernhard Schneider for collaboration on his farm.

SUPPLEMENTARY MATERIAL

The Supplementary Material for this article can be found online at: <https://www.frontiersin.org/articles/10.3389/fenvs.2022.856599/full#supplementary-material>

REFERENCES

- Ambus, P., Skiba, U., Drewer, J., Jones, S. K., Carter, M. S., Albert, K. R., et al. (2010). Development of an Accumulation-Based System for Cost-Effective Chamber Measurements of Inert Trace Gas Fluxes. *Eur. J. Soil Sci.* 61, 785–792. doi:10.1111/j.1365-2389.2010.01272.x
- Beare, M. H., Gregorich, E. G., and St-Georges, P. (2009). Compaction Effects on CO₂ and N₂O Production during Drying and Rewetting of Soil. *Soil Biol. Biochem.* 41, 611–621. doi:10.1016/j.soilbio.2008.12.024
- Biancalani, R., and Avagyan, A. (2014). *Towards Climate-Responsible Peatlands Management Series*. Rome, Italy: Food and Agriculture Organization of the United Nations.
- Blodau, C. (2002). Carbon Cycling in Peatlands - A Review of Processes and Controls. *Environ. Rev.* 10, 111–134. doi:10.1139/a02-004
- Bragg, O., Lindsay, R., Risager, M., Silvius, M., and Zingstra, H. (2013). Strategy And Action Plan for Mire and Peatland Conservation in central Europe: *Central European Peatland Project (CEPP)*. Wageningen: Wetlands International.
- Chapin, C. T., Bridgham, S. D., Pastor, J., and Updegraff, K. (2003). Nitrogen, Phosphorus, and Carbon Mineralization in Response to Nutrient and Lime Additions in Peatlands. *Soil Sci.* 168, 409–420. doi:10.1097/01.ss.0000075286.87447.5d
- Charteris, A. F., Chadwick, D. R., Thorman, R. E., Vallejo, A., Klein, C. A. M., Rochette, P., et al. (2020). Global Research Alliance N₂O Chamber Methodology Guidelines: Recommendations for Deployment and Accounting for Sources of Variability. *J. Environ. Qual.* 49, 1092–1109. doi:10.1002/jeq2.20126
- Clough, T. J., Kelliher, F. M., Wang, Y. P., and Sherlock, R. R. (2006). Diffusion of ¹⁵N-Labelled N₂O into Soil Columns: a Promising Method to Examine the Fate of N₂O in Subsoils. *Soil Biol. Biochem.* 38, 1462–1468. doi:10.1016/j.soilbio.2005.11.002
- Daly, E. J., and Hernandez-Ramirez, G. (2020). Sources and Priming of Soil N₂O and CO₂ Production: Nitrogen and Simulated Exudate Additions. *Soil Biol. Biochem.* 149, 107942. doi:10.1016/j.soilbio.2020.107942
- Danevčić, T., Mandić-Mulec, I., Stres, B., Stopar, D., and Hacin, J. (2010). Emissions of CO₂, CH₄ and N₂O from Southern European Peatlands. *Soil Biol. Biochem.* 42, 1437–1446. doi:10.1016/j.soilbio.2010.05.004
- Davidson, E. A., Keller, M., Erickson, H. E., Verchot, L. V., and Veldkamp, E. (2000). Testing a Conceptual Model of Soil Emissions of Nitrous and Nitric Oxides. *Bioscience* 50, 667–680. doi:10.1641/0006-3568(2000)050[0667:tacmos]2.0.co;2
- Dommain, R., Frolking, S., Jeltsch-Thömmes, A., Joos, F., Couwenberg, J., and Glaser, P. H. (2018). A Radiative Forcing Analysis of Tropical Peatlands before and after Their Conversion to Agricultural Plantations. *Glob. Change Biol.* 24, 5518–5533. doi:10.1111/gcb.14400
- Evans, C. D., Peacock, M., Baird, A. J., Artz, R. R. E., Burden, A., Callaghan, N., et al. (2021). Overriding Water Table Control on Managed Peatland Greenhouse Gas Emissions. *Nature* 593, 548–552. doi:10.1038/s41586-021-03523-1
- FAO (2017). *The Future of Food and Agriculture – Trends and Challenges*. Rome.
- Faostat (2019). Food and Agriculture Organisation of the United Nations. Available at: <https://www.fao.org/faostat/en/#data/GV>. (Accessed May 20, 2020).
- Ferré, M., Muller, A., Leifeld, J., Bader, C., Müller, M., Engel, S., et al. (2019). Sustainable Management of Cultivated Peatlands in Switzerland: Insights, Challenges, and Opportunities. *Land Use Policy* 87, 104019. doi:10.1016/j.landusepol.2019.05.038
- Flechar, C. R., Ambus, P., Skiba, U., Rees, R. M., Hensen, A., van Amstel, A., et al. (2007). Effects of Climate and Management Intensity on Nitrous Oxide Emissions in Grassland Systems across Europe. *Agric. Ecosyst. Environ.* 121, 135–152. doi:10.1016/j.agee.2006.12.024
- Flechar, C. R., Neftel, A., Jocher, M., Ammann, C., and Fuhrer, J. (2005). Bi-directional Soil/atmosphere N₂O Exchange over Two Mown Grassland Systems with Contrasting Management Practices. *Glob. Change Biol.* 11, 2114–2127. doi:10.1111/j.1365-2486.2005.01056.x
- Foen (2021). *Switzerland's Greenhouse Gas Inventory 1990–2019: National Inventory Report, CRF-Tables. Submission of April 2021 under the United Nations Framework Convention on Climate Change and under the Kyoto Protocol*. Bern: Federal Office for the Environment. Available at: <http://www.climate-reporting.ch>.
- Fuchs, K., Merbold, L., Buchmann, N., Bretscher, D., Brilli, L., Fitton, N., et al. (2020). Multimodel Evaluation of Nitrous Oxide Emissions from an Intensively Managed Grassland. *J. Geophys. Res. Biogeosci.* 125, e2019JG005261. doi:10.1029/2019jg005261
- Goldberg, S. D., Knorr, K.-H., and Gebauer, G. (2008). N₂O Concentration and Isotope Signature along Profiles Provide Deeper Insight into the Fate of N₂O in Soils†. *Isotopes Environ. Health Stud.* 44, 377–391. doi:10.1080/10256010802507433
- Günther, A., Barthelmes, A., Huth, V., Joosten, H., Jurasinski, G., Koesch, F., et al. (2020). Prompt Rewetting of Drained Peatlands Reduces Climate Warming Despite Methane Emissions. *Nat. Commun.* 11, 1644. doi:10.1038/s41467-020-15499-z
- Harris, E., Diaz-Pines, E., Stoll, E., Schloter, M., Schulz, S., Duffner, C., et al. (2021). Denitrifying Pathways Dominate Nitrous Oxide Emissions from Managed Grassland during Drought and Rewetting. *Sci. Adv.* 7 (6), eabb7118. doi:10.1126/sciadv.abb7118
- Harrison-Kirk, T., Beare, M. H., Meenken, E. D., and Condron, L. M. (2013). Soil Organic Matter and Texture Affect Responses to Dry/wet Cycles: Effects on Carbon Dioxide and Nitrous Oxide Emissions. *Soil Biol. Biochem.* 57, 43–55. doi:10.1016/j.soilbio.2012.10.008
- Hemes, K. S., Chamberlain, S. D., Eichelmann, E., Anthony, T., Valach, A., Kasak, K., et al. (2019). Assessing the Carbon and Climate Benefit of Restoring Degraded Agricultural Peat Soils to Managed Wetlands. *Agric. For. Meteorology* 268, 202–214. doi:10.1016/j.agrformet.2019.01.017
- Holtan-Hartwig, L., Dörsch, P., and Bakken, L. R. (2002). Low Temperature Control of Soil Denitrifying Communities: Kinetics of N₂O Production and Reduction. *Soil Biol. Biochem.* 34, 1797–1806. doi:10.1016/S0038-0717(02)00169-4
- IPCC (2014). in *2013 Supplement to the 2006 IPCC Guidelines for National Greenhouse Gas Inventories: Wetlands*. Editors T. Hiraishi, T. Krug, K. Tanabe, N. Srivastava, J. Baasansuren, M. Fukuda, et al. (Switzerland: IPCC). Available at: https://www.ipcc.ch/site/assets/uploads/2018/03/Wetlands_Supplement_Entire_Report.pdf.
- IPCC (2019). in *2019 Refinement to the 2006 IPCC Guidelines for National Greenhouse Gas Inventories*. Editors E. Calvo Buendia, K. Tanabe, A. Kranjc, J. Baasansuren, M. Fukuda, S. Ngarize, et al. (Switzerland: IPCC). Available at: <https://www.ipcc-nggip.iges.or.jp/public/2019r/vol4.html>.
- Kasimir, Å., He, H., Coria, J., and Nordén, A. (2018). Land Use of Drained Peatlands: Greenhouse Gas Fluxes, Plant Production, and Economics. *Glob. Change Biol.* 24, 3302–3316. doi:10.1111/gcb.13931
- Keller, T., Hüppi, R., and Leifeld, J. (2019). Relationship between Greenhouse Gas Emissions and Changes in Soil Gas Diffusivity in a Field experiment with Biochar and Lime. *J. Plant Nutr. Soil Sci.* 182, 667–675. doi:10.1002/jpln.201800538
- Knox, S. H., Sturtevant, C., Matthes, J. H., Koteen, L., Verfaillie, J., and Baldocchi, D. (2015). Agricultural Peatland Restoration: Effects of Land-Use Change on Greenhouse Gas (CO₂ and CH₄) Fluxes in the Sacramento-San Joaquin Delta. *Glob. Change Biol.* 21, 750–765. doi:10.1111/gcb.12745
- Kuang, W., Gao, X., Tenuta, M., Gui, D., and Zeng, F. (2019). Relationship between Soil Profile Accumulation and Surface Emission of N₂O: Effects of Soil Moisture and Fertilizer Nitrogen. *Biol. Fertil. Soils.* 55 (2), 97–107. doi:10.1007/s00374-018-01337-4
- Kuzyakov, Y., Friedel, J. K., and Stahr, K. (2000). Review of Mechanisms and Quantification of Priming Effects. *Soil Biol. Biochem.* 32, 1485–1498. doi:10.1016/S0038-0717(00)00084-5
- Lampe, C., Dittert, K., Sattelmacher, B., Wachendorf, M., Loges, R., and Taube, F. (2006). Sources and Rates of Nitrous Oxide Emissions from Grazed Grassland after Application of ¹⁵N-Labelled mineral Fertilizer and Slurry. *Soil Biol. Biochem.* 38, 2602–2613. doi:10.1016/j.soilbio.2006.03.016
- Leifeld, J. (2018). Distribution of Nitrous Oxide Emissions from Managed Organic Soils under Different Land Uses Estimated by the Peat C/N Ratio to Improve National GHG Inventories. *Sci. Total Environ.* 631–632, 23–26. doi:10.1016/j.scitotenv.2018.02.328
- Leifeld, J., and Menichetti, L. (2018). The Underappreciated Potential of Peatlands in Global Climate Change Mitigation Strategies. *Nat. Commun.* 9, 1071. doi:10.1038/s41467-018-03406-6
- Leppelt, T., Dechow, R., Gebbert, S., Freibauer, A., Lohila, A., Augustin, J., et al. (2014). Nitrous Oxide Emission Budgets and Land-Use-Driven Hotspots for

- Organic Soils in Europe. *Biogeosciences* 11, 6595–6612. doi:10.5194/bg-11-6595-2014
- Liu, B., Frostegård, Å., and Bakken, L. R. (2014). Impaired Reduction of N₂O to N₂ in Acid Soils Is Due to a Posttranscriptional Interference with the Expression of nosZ. *MBio* 5 (3), e01383–14. doi:10.1128/mBio.01383-14
- Liu, H., Wrage-Mönnig, N., and Lennartz, B. (2020). Rewetting Strategies to Reduce Nitrous Oxide Emissions from European Peatlands. *Commun. Earth Environ.* 1, 1–7. doi:10.1038/s43247-020-00017-2
- Marushchak, M. E., Pitkämäki, A., Koponen, H., Biasi, C., Seppälä, M., and Martikainen, P. J. (2011). Hot Spots for Nitrous Oxide Emissions Found in Different Types of Permafrost Peatlands. *Glob. Chang. Biol.* 17, 2601–2614. doi:10.1111/j.1365-2486.2011.02442.x
- Meng, L., Ding, W., and Cai, Z. (2005). Long-term Application of Organic Manure and Nitrogen Fertilizer on N₂O Emissions, Soil Quality and Crop Production in a sandy Loam Soil. *Soil Biol. Biochem.* 37, 2037–2045. doi:10.1016/j.soilbio.2005.03.007
- Merbold, L., Decock, C., Eugster, W., Fuchs, K., Wolf, B., Buchmann, N., et al. (2021). Are There Memory Effects on Greenhouse Gas Emissions (CO₂, N₂O and CH₄) Following Grassland Restoration? *Biogeosciences* 18 (4), 1481–1498. doi:10.5194/bg-2020-141
- Nadeem, S., Bakken, L. R., Frostegård, Å., Gaby, J. C., and Dörsch, P. (2020). Contingent Effects of Liming on N₂O-Emissions Driven by Autotrophic Nitrification. *Front. Environ. Sci.* 8, 598513. doi:10.3389/fenvs.2020.598513
- Neftel, A., Blatter, A., Schmid, M., Lehmann, B., and Tarakanov, S. V. (2000). An Experimental Determination of the Scale Length of N₂O in the Soil of a Grassland. *J. Geophys. Res.* 105, 12095–12103. doi:10.1029/2000jd900088
- Ojanen, P., and Minkinen, K. (2020). Rewetting Offers Rapid Climate Benefits for Tropical and Agricultural Peatlands but Not for Forestry-Drained Peatlands. *Glob. Biogeochem. Cycles* 34. doi:10.1029/2019gb006503
- Pärn, J., Verhoeven, J. T. A., Butterbach-Bahl, K., Dise, N. B., Ullah, S., Aasa, A., et al. (2018). Nitrogen-rich Organic Soils under Warm Well-Drained Conditions Are Global Nitrous Oxide Emission Hotspots. *Nat. Commun.* 9, 1135. doi:10.1038/s41467-018-03540-1
- Perveen, N., Barot, S., Maire, V., Cotofofo, M. F., Shahzad, T., Blagodatkaya, E., et al. (2019). Universality of Priming Effect: An Analysis Using Thirty Five Soils with Contrasted Properties Sampled from Five Continents. *Soil Biol. Biochem.* 134, 162–171. doi:10.1016/j.soilbio.2019.03.027
- Prather, M. J., Hsu, J., DeLuca, N. M., Jackman, C. H., Oman, L. D., Douglass, A. R., et al. (2015). Measuring and Modeling the Lifetime of Nitrous Oxide Including its Variability. *J. Geophys. Res. Atmos.* 120, 5693–5705. doi:10.1002/2015JD023267
- Priemé, A., and Christensen, S. (2001). Natural Perturbations, Drying–Wetting and Freezing–Thawing Cycles, and the Emission of Nitrous Oxide, Carbon Dioxide and Methane from Farmed Organic Soils. *Soil Biol. Biochem.* 33, 2083–2091. doi:10.1016/S0038-0717(01)00140-7
- Ravishankara, A. R., Daniel, J. S., and Portmann, R. W. (2009). Nitrous Oxide (N₂O): The Dominant Ozone-Depleting Substance Emitted in the 21st Century. *Science* 326, 123–125. doi:10.1126/science.1176985
- Rihm, B., and Künzle, T. (2019). *Mapping Nitrogen Deposition 2015 for Switzerland. Technical Report on the Update of Critical Loads and Exceedance, Including the Years 1990, 2000, 2005 and 2010.* Switzerland: Bern. Available at: <https://www.bafu.admin.ch>.
- Roman-Perez, C. C., and Hernandez-Ramirez, G. (2020). Sources and Priming of Nitrous Oxide Production across a Range of Moisture Contents in a Soil with High Organic Matter. *J. Environ. Qual.* 50, 94–109. doi:10.1002/jeq2.20172
- Schindler, U., and Müller, L. (2001). “Rehabilitation of the Soil Quality of a Degraded Peat Site,” in *10th International Soil Conservation*. Editors S. R. H. DE and G. C. S. M (West Lafayette, USA: Organization Meeting Purdue University), 648–654.
- Schjøning, P., Thomsen, I. K., Moldrup, P., and Christensen, B. T. (2003). Linking Soil Microbial Activity to Water- and Air-phase Contents and Diffusivities. *Soil Sci. Soc. Am. J.* 67, 156–165. doi:10.2136/sssaj2003.1560
- Schleusner, P., Lammirato, C., Tierling, J., Lebender, U., and Rütting, T. (2018). Primed N₂O Emission from Native Soil Nitrogen: A ¹⁵N-tracing Laboratory experiment. *J. Plant Nutr. Soil Sci.* 181, 621–627. doi:10.1002/jpln.201700312
- Senbayram, M., Chen, R., Budai, A., Bakken, L., and Dittert, K. (2012). N₂O Emission and the N₂O/(N₂O+N₂) Product Ratio of Denitrification as Controlled by Available Carbon Substrates and Nitrate Concentrations. *Agric. Ecosyst. Environ.* 147, 4–12. doi:10.1016/j.agee.2011.06.022
- Stehfest, E., and Bouwman, L. (2006). N₂O and NO Emission from Agricultural fields and Soils under Natural Vegetation: Summarizing Available Measurement Data and Modeling of Global Annual Emissions. *Nutr. Cycl. Agroecosyst* 74, 207–228. doi:10.1007/s10705-006-9000-7
- Syakila, A., and Kroeze, C. (2011). The Global Nitrous Oxide Budget Revisited. *Greenhouse Gas Meas. Management* 1, 17–26. doi:10.3763/ghgmm.2010.0007
- Tanneberger, F., Moen, A., Joosten, H., and Nilsen, N. (2017). The Peatland Map Of Europe. *Mires and Peat* 19, 1–17. doi:10.19189/Map.2016.OMB.264
- Thilakarathna, S. K., and Hernandez-Ramirez, G. (2021). Primings of Soil Organic Matter and Denitrification Mediate the Effects of Moisture on Nitrous Oxide Production. *Soil Biol. Biochem.* 155, 108166. doi:10.1016/j.soilbio.2021.108166
- Tian, H., Yang, J., Xu, R., Lu, C., Canadell, J. G., Davidson, E. A., et al. (2019). Global Soil Nitrous Oxide Emissions since the Preindustrial Era Estimated by an Ensemble of Terrestrial Biosphere Models: Magnitude, Attribution, and Uncertainty. *Glob. Change Biol.* 25, 640–659. doi:10.1111/gcb.14514
- Tiemeyer, B., Albiac Borraz, E., Augustin, J., Bechtold, M., Beetz, S., Beyer, C., et al. (2016). High Emissions of Greenhouse Gases from Grasslands on Peat and Other Organic Soils. *Glob. Change Biol.* 22, 4134–4149. doi:10.1111/gcb.13303
- Wang, Y., Paul, S. M., Jocher, M., Espic, C., Alewell, C., Szidat, S., et al. (2021). Soil Carbon Loss from Drained Agricultural Peatland after Coverage with mineral Soil. *Soil. Total Environ.* 800, 149498. doi:10.1016/j.scitotenv.2021.149498
- Weslien, P., Kasimir Klemetsson, Å., Börjesson, G., and Klemetsson, L. (2009). Strong pH Influence on N₂O and CH₄ Fluxes from Forested Organic Soils. *Eur. J. Soil Sci.* 60, 311–320. doi:10.1111/j.1365-2389.2009.01123.x
- Wüst-Galley, C., Grünig, A., and Leifeld, J. (2020). Land Use-Driven Historical Soil Carbon Losses in Swiss Peatlands. *Landscape Ecol.* 35, 173–187. doi:10.1007/s10980-019-00941-5
- Wüst-Galley, C., Grünig, A., and Leifeld, J. (2015). Locating Organic Soils for the Swiss Greenhouse Gas Inventory. *Agroscopie Sci.*, 1–100.
- Yu, Z., Loisel, J., Brosseau, D. P., Beilman, D. W., and Hunt, S. J. (2010). Global Peatland Dynamics since the Last Glacial Maximum. *Geophys. Res. Lett.* 37, a–n. doi:10.1029/2010gl043584

Conflict of Interest: The authors declare that the research was conducted in the absence of any commercial or financial relationships that could be construed as a potential conflict of interest.

Publisher’s Note: All claims expressed in this article are solely those of the authors and do not necessarily represent those of their affiliated organizations, or those of the publisher, the editors, and the reviewers. Any product that may be evaluated in this article, or claim that may be made by its manufacturer, is not guaranteed or endorsed by the publisher.

Copyright © 2022 Wang, Paul, Jocher, Alewell and Leifeld. This is an open-access article distributed under the terms of the Creative Commons Attribution License (CC BY). The use, distribution or reproduction in other forums is permitted, provided the original author(s) and the copyright owner(s) are credited and that the original publication in this journal is cited, in accordance with accepted academic practice. No use, distribution or reproduction is permitted which does not comply with these terms.